Adsorption, Gas-Sensing, and Optical Properties of Molecules on a Diazine Monolayer: A First-Principles Study

Xiaojiao Wang, Yongliang Yong,* Wenwen Yang, Aodi Zhang, Xiangyi Xie, Peng Zhu, and Yanmin Kuang

ACCESS | Metrics & More | Article Recommendations

ABSTRACT: Using first-principles calculations, the structural, electronic, and optical properties of CO_2, CO, N_2O, CH_4, H_2, N_2, O_2, NH_3, acetone, and ethanol molecules adsorbed on a diazine monolayer were studied to develop the application potential of the diazine monolayer as a room-temperature gas sensor for detecting acetone, ethanol, and NH_3. We found that these molecules are all physically adsorbed on the diazine monolayer with weak adsorption strength and charge transfer between the molecules and the monolayer, but the physisorption of only NH_3, acetone, and ethanol remarkably modified the electronic properties of the diazine monolayer, especially for the obvious change in electric conductivity, showing that the diazine monolayer is highly sensitive to acetone, NH_3, and ethanol. Further, the adsorption of NH_3, acetone, and ethanol molecules remarkably modifies, in varying degrees, the optical properties of the diazine monolayer, such as work function, absorption coefficient, and the reflectivity, whereas adsorption of other molecules has infinitesimal influence. The different adsorption behaviors and influences of the electronic and optical properties of molecules on the monolayer show that the diazine monolayer has high selectivity to NH_3, acetone, and ethanol. The recovery time of NH_3, acetone, and ethanol molecules is, respectively, 1.2 μs, 7.7 μs, and 0.11 ms at 300 K. Thus, the diazine monolayer has a high application potential as a room-temperature acetone, ethanol, and NH_3 sensor with high performance (high selectivity and sensitivity, and rapid recovery time).
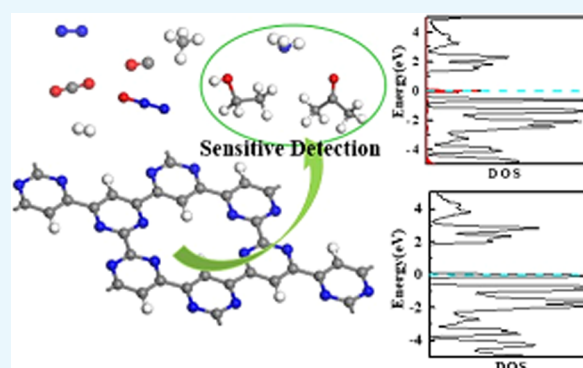
1. INTRODUCTION

Since worldwide air pollution through contamination by a variety of gases that are toxic, harmful, flammable, and explosive, such as volatile organic compounds (VOCs), ethanol (C_2H_6O), formaldehyde (HCHO), nitrogen oxides (NO_x), acetone (C_3H_6O), ammonia (NH_3), sulfur oxides (SO_x), and carbon monoxide (CO), is one of the major threats to human life and the environment, detecting and sensing polluting gases plays a crucial role in controlling of the chemical processes in industries, indoor air quality supervision, space missions, and medical and environmental monitoring. Hence, designing and researching novel gas-sensor materials with high sensitivity and selectivity has paramount importance in the detection and monitoring of polluting gases in the modern era.[1−7] In the past decades, a tremendous amount of two-dimensional (2D) nanomaterials,[6−16] such as graphene and related 2D crystals, phosphorene, transition metal dichalcogenides, and MXenes, have been extensively used as gas-sensing materials owing to their ultrahigh specific surface area, strong surface activities, high mobility, excellent thermal and electrical conductivities, and high chemical and thermodynamic stability.

Previous studies had shown that pure graphene is not suitable as a gas sensor due to the lack of a band gap, but that modification with doping and defects can improve observably the gas-sensing performance of graphene.[7,8,11,14−20] Recently, the excellent structural, electronic, mechanical, and thermodynamic properties of graphyne (i.e., nanoporous graphene), and graphene analogs including intrinsic uniformly distributed pores, thereby producing membranes with a large surface area, have made it an appealing candidate for use in gas sensors and gas separation.[21−31] For example, Shaban et al.[29] designed a 2D nanoporous graphene oxide (NGO) using the modified Hummer method and the spray pyrolysis technique, and found that NGO shows high selectivity and rapid response to sense CO_2, H_2, and C_2H_2 gases. Recently, Barone and Moses[32] used molecular units (benzene, single heteroatom heterocycles,
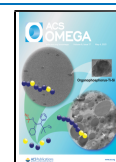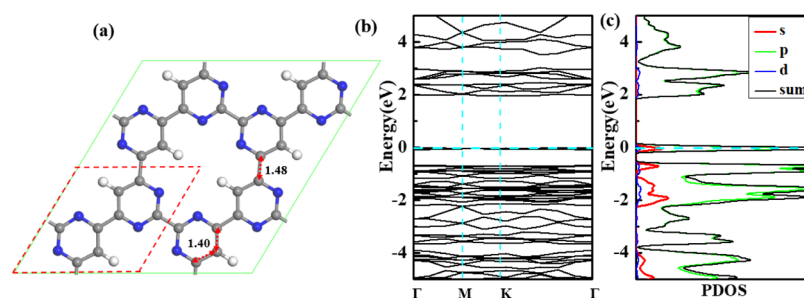
Figure 1. (a) Optimized configuration of the diazine monolayer, (b, c) the corresponding band structure and partial density of states (PDOS), respectively. The bond lengths between the C atoms are given as red lines with arrows in angstrom. The blue, gray, and white balls represent N, C, and H atoms, respectively. The Fermi level energy is set to zero.
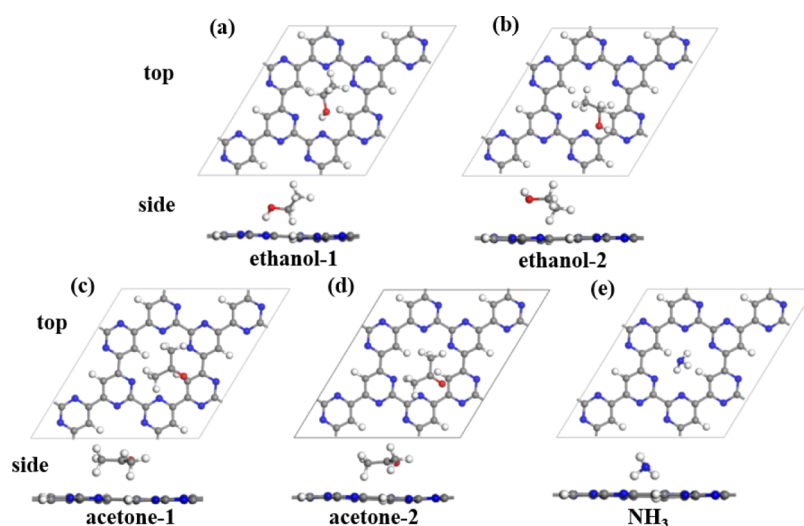

Figure 2. Top and side views of the most stable structures of the diazine monolayer with molecular adsorption: (a, b) ethanol; (c, d) acetone; and (e) NH_3. The molecule−monolayer system is labeled by the molecule name. The red balls represent O atoms.

borazine, 1,3-diazine, and 1,3,5-triazine) as building blocks to design a variety of nanoporous graphene-like monolayers, and further investigated their structural properties and stabilities using density functional theory (DFT) methods. Their results indicated that diazine monolayers, which are formed by seamlessly connected diazine molecules, have the highest stability among all studied compounds and have wide-band-gap semiconductor characteristics. In the most stable structure of the diazine monolayer, the C and N atoms have similar bonding characteristics with the C_2N monolayer, which is composed of two benzene rings bridged by pyrazine rings in which two nitrogen atoms face each other,[17,18,33−38] and the structural difference between the diazine and C_2N monolayers is that one C atom binds to a H atom and thereby forms sp^2 hybridization in the diazine monolayer. As reported in a previous work,[32] as the diazine monolayer has advantages such as ultrahigh specific surface area and semiconducting properties with wide band-gap width, it is expected that the diazine monolayer, which would be similar to the C−N 2D nanomaterials,[17−20,33−41] has promising potential applications in ion batteries, (photo-) catalysts, gas capture and storage, gas sensors, and so on. More interestingly, it had been demonstrated that the C_2N monolayer as a gas sensor has excellent gas-sensing properties such as high sensitivity and selectivity for detection of gaseous pollutants.[17,18,35] The fact that the analogous structure C_2N is a good candidate for a gas sensor indicates that the diazine monolayer can be expected to

show excellent gas-sensing performance. Therefore, following the progress of investigations on C_xN_y monolayers as gas-sensing materials,[17−20,35] as well as given the facts such as the unique geometric structure, stability, and semiconducting properties of the diazine monolayer, it is highly expected that the diazine monolayer will be a promising potential for applications in gas-sensing materials.

In this study, using first-principles calculations based on DFT, we investigated the application potential of the diazine monolayer as a gas sensor for detection of toxic gases. To this end, we studied systemically the adsorption behaviors, and electronic and gas-sensing properties of molecules (CO_2, CO, N_2O, CH_4, H_2, N_2, O_2, NH_3, acetone, and ethanol) on the diazine monolayer in terms of their adsorption energy, charge transfer, changes in band structures and density of states (DOS), work function, and optical properties. Our results indicate that the diazine monolayer as a room-temperature acetone, ethanol, and NH_3 sensor has high selectivity and sensitivity and rapid recovery time. Further, the adsorption of three molecules remarkably modifies the optical properties of the pure diazine monolayer, such as work function, absorption coefficient, and reflectivity, whereas adsorption of the other molecules has infinitesimal influence. It is noted that since Barone et al. predicted the stable structure of the diazine monolayer in 2019,[32] it is not like other C−N monolayers such as C_2N and C_3N,[17−20,33−41] which have received much attention due to their properties and applications after their
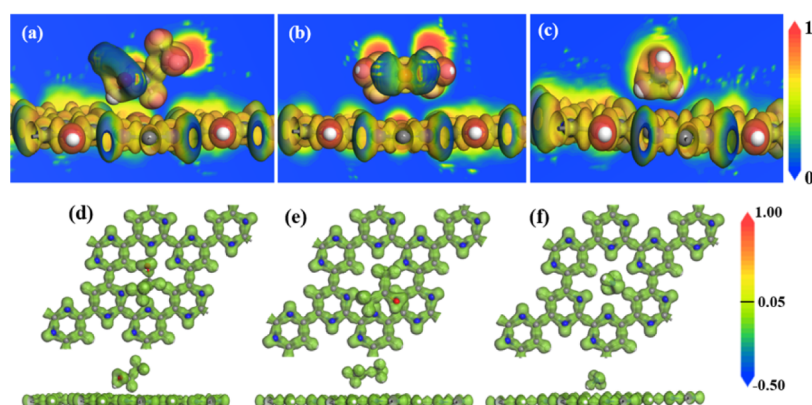
Figure 3. ELF plots (a−c) and electron density difference (d−f) for the most stable configurations for (a, d) ethanol; (b, e) acetone; and (c, f) NH$_3$ adsorbed on the diazine monolayer, respectively.

Table 1. Adsorption Energy (E_{ads}), Charge Transferred from the Monolayer to Molecule (ΔQ), the Shortest Distance between the Molecule and Monolayer (D), Band-Gap Widths (E_g), Work Function (Φ), and the Recovery Time (τ) for the Structures of Ethanol, Acetone, and NH$_3$ Adsorbed on the Diazine Monolayer

system	E_{ads} (eV)	ΔQ (e)	D (Å)	E_g (eV)	Φ (eV)	τ (s)
ethanol-1	−0.479	−0.145	1.254	1.387	5.687	1.1×10^{-4}
ethanol-2	−0.329	−0.052	1.382	1.958	6.068	3.4×10^{-7}
acetone-1	−0.413	−0.093	1.774	1.371	5.578	7.7×10^{-6}
acetone-2	−0.410	−0.076	1.735	1.444	5.632	8.7×10^{-6}
NH$_3$	−0.362	−0.077	1.339	1.415	5.660	1.2×10^{-6}

prediction and synthesis. To our knowledge, there are few reports on the investigations of the properties and applications of the diazine monolayer. We hope that our work could further motivate people to pay close attention to the properties, potential applications, and experimental synthesis and verification of this material.

2. RESULTS AND DISCUSSION

We investigated firstly the 2 × 2 × 1 supercell mode of the diazine monolayer with and without molecular adsorption, as shown in Figure 1a. After full optimization, we found that the calculated lattice parameters of the optimized diazine monolayer are a = 7.08 Å and b = 7.37 Å, and the angle between the lattice vectors is 58.7°. There are two bond lengths for C−C bonds: one is 1.40 Å in the diazine six-membered rings, and the other is 1.48 Å in the C−C bonds bridging the diazine six-membered rings, which are shown in Figure 1a. The lengths of the C−N and C-H bonds are 1.34 and 1.09 Å, respectively. The diazine monolayer is a semiconductor with a direct band-gap value of 1.953 eV at generalized gradient approximation Perdew−Burke−Ernzerhof (GGA-PBE) level as shown in Figure 1b, which is smaller than that obtained with the HSE functional,[32] as the GGA-PBE functional often underestimates the band gaps of materials. Further, it can be seen from the DOS as shown in Figure 1c that the contribution of the 2p states of N and C atoms has a strong influence on the valence band and conduction band. These results are also in good agreement with previous reports.[32]

To study the gas-sensing performance of the diazine monolayer, we then investigated the adsorption behaviors of the molecules (CO$_2$, CO, N$_2$O, CH$_4$, H$_2$, N$_2$, O$_2$, NH$_3$, acetone, and ethanol) on the diazine monolayer. The optimized most stable configurations of each molecule adsorbed on the diazine monolayer are shown in Figures 2

and 3, and the related results are listed in Tables 1 and 2, respectively. We firstly explored the adsorption of ethanol,

Table 2. Adsorption Energy (E_{ads}), Charge Transferred from the Monolayer to Molecule (ΔQ), the Shortest Distance between the Molecule and Monolayer (D), Band-Gap Widths (E_g), Work Function (Φ), and the Recovery Time (τ) for the Structures of the Molecules Adsorbed on the Diazine Monolayer

system	E_{ads} (eV)	ΔQ (e)	D (Å)	E_g (eV)	Φ (eV)	τ (s)
CO$_2$	−0.230	0.003	2.051	1.948	6.150	7.3×10^{-9}
CO	−0.149	0.001	2.269	1.957	6.150	3.2×10^{-10}
N$_2$O	−0.213	0.019	2.181	1.953	6.150	3.8×10^{-9}
CH$_4$	−0.211	−0.077	1.629	1.955	6.150	3.5×10^{-9}
H$_2$	−0.075	−0.021	2.183	1.956	6.150	1.8×10^{-11}
N$_2$	−0.129	0.007	2.022	1.964	6.150	1.5×10^{-10}
O$_2$	0.303		2.984			

acetone, and NH$_3$ on the diazine monolayer, and the most stable configurations are shown in Figure 2. For ethanol adsorption, we found that the ethanol molecule is located at the top of the monolayer pores, which is energetically favorable with an E_{ads} of −0.479 eV and results in charge (0.145 e) transfer from the diazine monolayer to the ethanol molecule, leading to the positively charged ethanol molecule. Further, the adsorption strength of ethanol on the diazine monolayer decreases when the ethanol molecule deviates from the top site of the monolayer pore (see Figure 2b), as the second stable structure for ethanol adsorption has an E_{ads} of −0.329 eV. We also found that the acetone and NH$_3$ molecules are also located at the top of the monolayer pores to form the most favorable configurations as shown in Figure 2c,e, with an E_{ads} of −0.413 and −0.362 eV, respectively. The adsorption of acetone and NH$_3$ molecules leads to very little transfer of
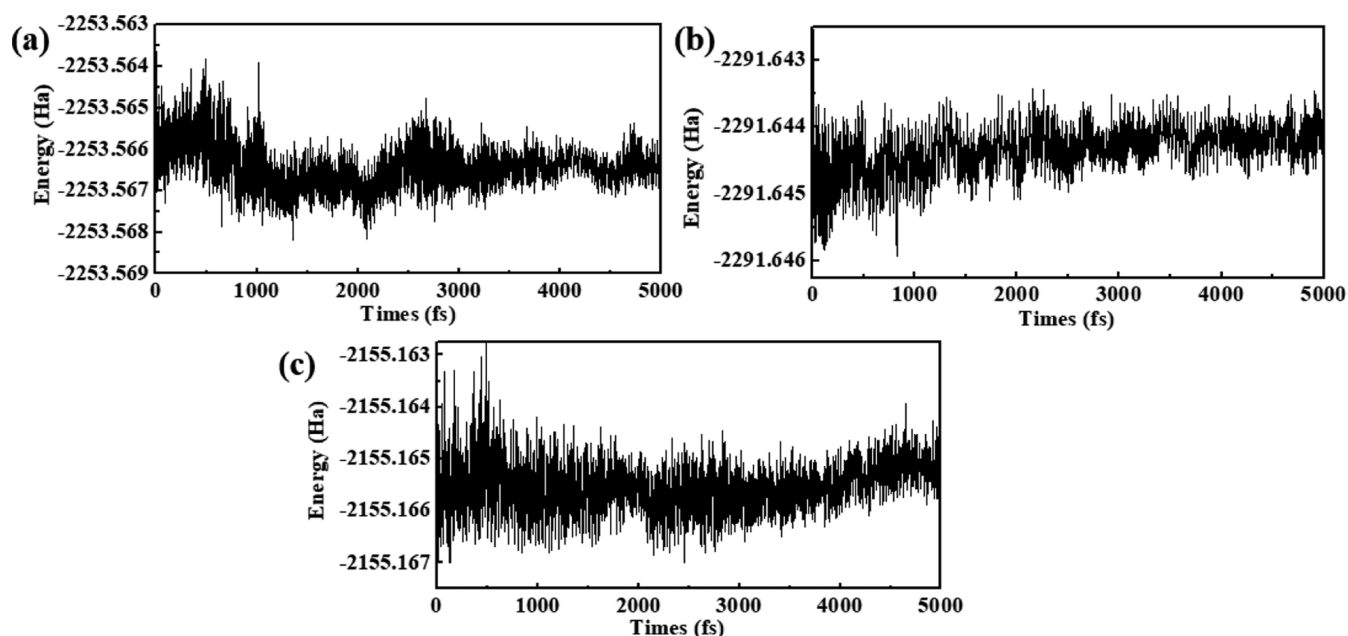
Figure 4. Variation in the total energy (Ha) of the most stable configuration of (a) ethanol; (b) acetone; and (c) NH_3 adsorbed on the diazine monolayer as a function of time at 300 K.

charges between acetone and the NH_3 molecule and diazine monolayer, that is, 0.093 and 0.077 e charge is transferred from the diazine monolayer to acetone and the NH_3 molecule, respectively, which is very different from the case of ethanol adsorption. This may indicate that the small transferred charge between the monolayer and acetone and the NH_3 molecule would have little influence on the electronic properties of the diazine monolayer due to acetone and NH_3 adsorption. Moreover, it is found that ethanol adsorption results in the largest charge transfer among the considered molecules and also has the largest adsorption strength, indicating that the transferred charge between ethanol and the diazine monolayer plays an indispensable role in the adsorption process of ethanol on the monolayer. Further, it is different from the ethanol adsorption in that the acetone adsorption sites deviating from the top of pore do not induce any obvious change in adsorption strength (Table 1). In addition, we found that the three molecules are not bonded with the diazine monolayer and induce an unapparent charge transfer as shown in Table 1. Based on these analyses, it may be concluded that these three molecules are all physisorbed on the diazine monolayer. To clarify the physisorption of molecules on the monolayer, we also investigated the electron localization function (ELF), which is an efficient method to understand the features of chemical bonding, the lone electron pairs (nonbonding electron pairs), and (non)covalent interactions between the molecules and the monolayer,[42−44] and the results of the analysis of the characteristics of chemical bonding for the molecule adsorption system are similar to those of the noncovalent interactions analysis.[39,40] The ELF function has values between 0 and 1, which represents delocalization and the perfect localization features of the covalent bonding or the lone electron pairs, respectively. The ELF plots for the adsorption of the considered three molecules are presented in Figure 3a−c. We found that the ELF values between the atoms of three molecules and the nearest atoms of the diazine monolayer are all less than 0.5, nearly tending to zero, indicating that no chemical bonds between those molecules

and the diazine monolayer are formed, that is, there are noncovalent interactions between the three molecules and the diazine monolayer, which is positive evidence for the physisorption of NH_3, acetone, and ethanol molecules on the diazine monolayer. Further, the electron density differences (EDD) of the most stable structures for NH_3, acetone, and ethanol adsorbed on the diazine monolayer were calculated and are illustrated in Figure 3d,e, which provides us some positive information on the electron-available or -depleted regions. The red and blue regions represent, respectively, the increase and decrease of the electron density in Figure 3d,e. The existence of electron occupancy locations throughout the molecule−monolayer systems could be confirmed via the positive value of EDD (0.05 Å^{-3}). When ethanol adsorbs on the diazine monolayer, a very few electrons are transferred from the molecule to the monolayer; however, few electrons can be transferred between the diazine monolayer and NH_3 (acetone) molecule, which is in good agreement with the Hirshfeld charge analysis. In order to study the thermodynamic stability of the diazine monolayer with NH_3, acetone, and ethanol adsorption, we carried out molecular dynamics (MD) simulations in the framework of the Born−Oppenheimer concept (BOMD) within the NVT ensemble for the most stable structures of NH_3, acetone, and ethanol adsorbed on the diazine monolayer. The temperature was controlled using a Nosé−Hoover chain thermostat. We set simulations of 5 ps with a time step of 1 fs at a constant temperature of 300 K. Figure 4 shows the vitiation of the total energies for the structures during the simulations. We found that there is no structural deformation for the most stable structures of NH_3, acetone, and ethanol adsorbed on the diazine monolayer after 5 ps. Furthermore, the total energies of the most stable structures of NH_3, acetone, and ethanol adsorbed on the diazine monolayer vibrate in a very small energy range during the simulations, which provides the evidence for the thermal stability of the calculated structures.

We also investigated the effects of molecule adsorption on the structural properties of the pure diazine monolayer. We
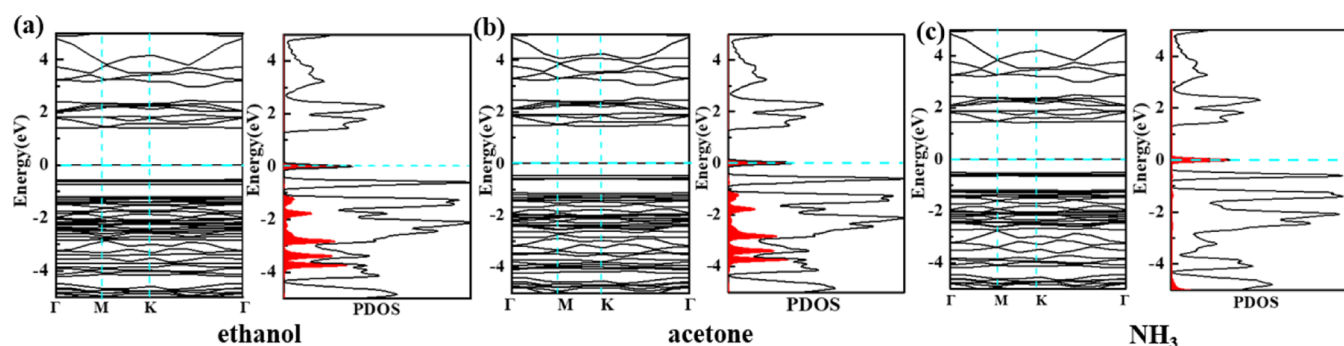
Figure 5. Bband structures and partial density of states (PDOS) for the most stable configuration of (a) ethanol; (b) acetone; and (c) NH_3 adsorbed on the diazine monolayer. The LDOS of the molecules is shown by the red filled area under the DOS curve. The Fermi level is set to zero.
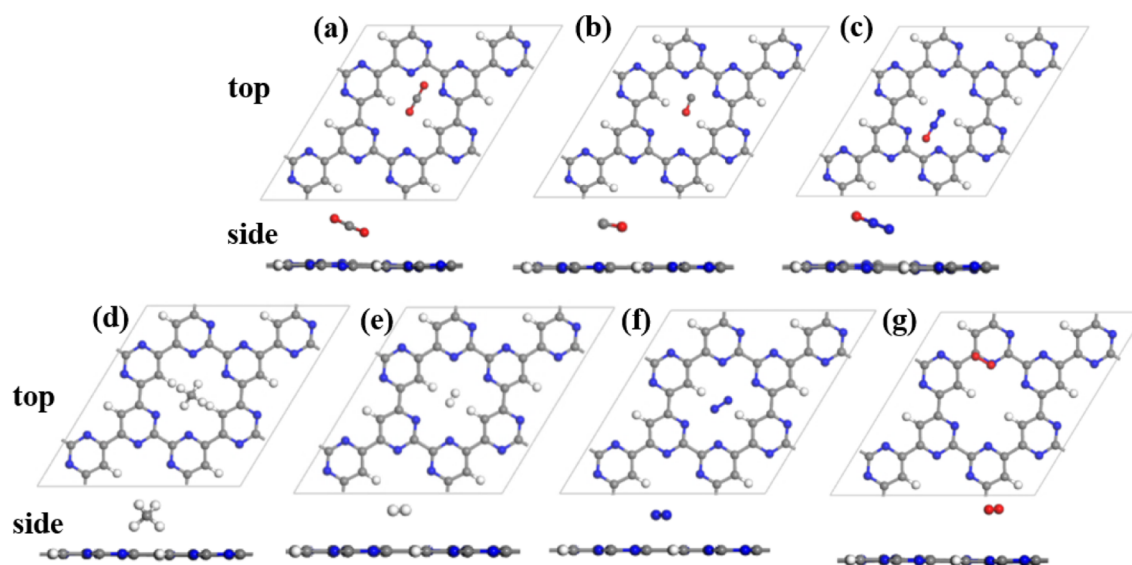

Figure 6. Top and side views of the optimized most stable structures of the diazine monolayer with molecular adsorption: (a) CO_2; (b) CO; (c) N_2O; (d) CH_4; (e) H_2; (f) N_2; and (g) O_2. The molecule−monolayer systems are labeled by the molecule name.

found that the bond lengths of C−C, C−N, and C-H bonds, and the angles of C−C−C, N−C−C, C−N−C, and H−C−C in the pure diazine monolayer were nearly unchanged due to the adsorption of molecules. More importantly, the diazine monolayer still keeps the planar structure after molecule adsorption. These results indicate that the physisorption of NH_3, acetone, and ethanol molecules hardly results in any structural deformation for the diazine monolayer, indicating that the diazine monolayer keeps structural stability even after molecule adsorption, which is a key requirement for gas sensing. We noted that all possible adsorption sites for NH_3, acetone, and ethanol molecule adsorption on the diazine monolayer were considered in this work; however, we just obtained the most stable physisorption configurations for these molecules on the monolayer, and no chemisorption states for these molecules on the diazine monolayer were found, which is very similar to the cases of molecule adsorption on the C_xN (x = 2, 3) monolayers.[17−20]

To gain more insight into the interactions between the molecules (NH_3, acetone, and ethanol) and the diazine monolayer, we calculated the electronic structures of the most stable structures for the three molecules adsorbed on the diazine monolayer. It is well known that the GGA-PBE functional underestimates the band gap of materials, but it still considerably describes the characteristics of electronic

structures. The band structures and density of states (DOS) combined with local DOS (LDOS) projected for the molecules are presented in Figure 5. In comparison with the DOS and band structure of the pure diazine monolayer, we found that the adsorption of ethanol, acetone, and NH_3 molecules produces certain impurity states that are located in the band gap and makes the Fermi level cross these states. The gas adsorption thus decreases the original band gap. As discussed below, the feature of narrowing the band gap is important for application in gas sensors. For ethanol adsorption as shown in Table 1, we found that the values of the band gap and transferred charge decrease as the adsorption strength decreases. We further explored the adsorption of CO_2, CO, N_2O, CH_4, H_2, N_2, and O_2 molecules on the diazine monolayer; the most stable structures of each molecule adsorbed on the monolayer are shown in Figure 6 with the calculated results summarized in Table 2. For O_2 adsorption, the O_2 molecule has an unfavorable E_{ads} of 0.303 eV and the adsorption process is endothermic, which suggests that the diazine monolayer is highly inert toward O_2 gas in ambient conditions, which is very similar to the adsorption of O_2 molecule on ZnO[45] and GaN[46] nanowires, and the GaN monolayer.[47] For the other molecules, the adsorption energies are all larger than −0.24 eV and the charge transfers are quite small, which indicates that the adsorption strength for these
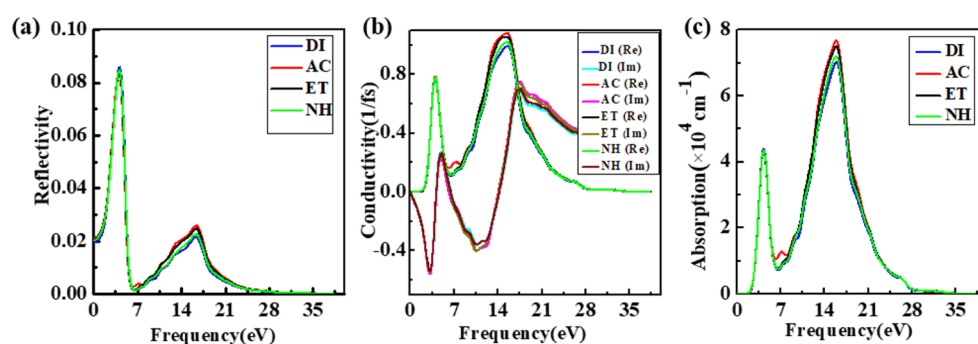
Figure 7. (a) Reflectivity, (b) the real dielectric function (Re) and imaginary dielectric function (Im), and (c) the absorption coefficient of the pristine and gas-molecule-adsorbed diazine monolayer. DI, AC, ET, and NH represent the system of the pure diazine monolayer, acetone, ethanol, and NH_3 adsorption on the monolayer, respectively.

molecules is so weak that they may have no influence on the electronic properties of the diazine monolayer. As expected, it can be seen from Table 2 that the adsorption of CO_2, CO, N_2O, CH_4, H_2, and N_2 molecules barely changes the electronic and optical properties of the diazine monolayer. Further, it can be seen from Tables 1 and 2 that ethanol, acetone, and NH_3 adsorption has the largest adsorption strength (i.e., the largest absolute value of adsorption energy) and shows the most obvious changes of band gaps among all of the considered molecules, indicating that the larger adsorption strength would result in a larger change in the band gaps of the monolayer.

Then, we studied the application potential of the diazine monolayer as a good gas sensor for ethanol, acetone, and NH_3 detection. For the gas-sensing properties, we mainly analyzed the stability, work function, sensitivity, selectivity, and recovery time of the diazine monolayer in the sensing process. Previous studies have demonstrated that the diazine monolayer is energetically and dynamically stable. In addition, adsorption of the molecules does not induce any structural deformation in the monolayer (see Figures 2 and 6), further indicating its stability.

The work function (Φ), which is described as $\Phi = E_{vac} - E_F$, where E_{vac} and E_F are the vacuum energy and Fermi energy, respectively, is an important parameter to evaluate the potential of materials as gas sensors.[17,19,41] The calculated work function of the diazine monolayer is 6.150 eV. The work functions of the molecules on the monolayer are listed in Tables 1 and 2. The adsorption of ethanol, acetone, and NH_3 leads to the values of Φ for the diazine monolayer decreasing to 5.687, 5.578, and 5.660 eV (i.e., 7.5, 9.3, and 7.2% variation), respectively. However, the work function remains almost unchanged for the physical adsorption of CO_2, CO, N_2O, CH_4, H_2, and N_2 molecules on the diazine monolayer. These results indicate that the selective adsorption of ethanol, acetone, and NH_3 can efficiently tune the work function of the diazine monolayer, which endows it a promising potential for work function-type gas sensors. Further, the change in the electric conductivity of materials before and after molecule adsorption can be used to evaluate the sensitivity of the materials to a certain gas. The electric conductivity (σ) is described as $\sigma \propto \exp\left(\frac{-E_g}{2kT}\right)$,[48] where E_g is the band gap, k Boltzmann's constant, and T the temperature. The change in band gap for the most stable configurations of ethanol, acetone, and NH_3 adsorption on the diazine monolayer is from 1.953 eV of the pure diazine monolayer to 1.387, 1.371, and 1.415 eV, respectively, that is to say, the variation of band gap

is 29.0, 29.8, and 27.6% for ethanol, acetone, and NH_3 adsorption, respectively. The remarkable change in band gap inevitably leads to the obvious change in electric conductivity due to ethanol, acetone, and NH_3 adsorption, indicating that the diazine monolayer as a gas sensor has a high sensitivity for detection of ethanol, acetone, and NH_3 gases. On the contrary, the very weak physisorption of CO_2, CO, N_2O, CH_4, H_2, and N_2 molecules alters hardly the band gap of the diazine monolayer, which indicates that the diazine monolayer has quite low sensitivity (or insensitivity) to these gases.

Further, as discussed above, the weak physisorption of CO_2, CO, N_2O, CH_4, H_2, and N_2 molecules does not change basically the electronic and optical (work function) properties of the diazine monolayer, but the adsorption of ethanol, acetone, and NH_3 has various degrees of influence on the electronic properties of the diazine monolayer, which indicates that the diazine monolayer is highly selective for ethanol, acetone, and NH_3 gas, and can easily distinguish these three gases from the compounds of CO_2, CO, N_2O, CH_4, H_2, and N_2. Further, we could use the optical properties of ethanol, acetone, and NH_3 on the diazine monolayer to differentiate them from each other, as the adsorption leads to different optical properties. We thus calculated the optical properties such as reflectivity, the real and imaginary dielectric functions, and absorption coefficient, which are shown in Figure 7. It is found from Figure 7 that there are new peaks added in the reflectivity, real dielectric function, and absorption coefficient curves, which are mainly located at about 5.5×10^4 cm^{-1} in the deep ultraviolet (UV) region (about 7.0 eV), due to the adsorption of acetone, indicating that we can differentiate acetone from ethanol and NH_3 by measuring the newly added peaks in the optical properties mentioned above. More interestingly, the adsorption of ethanol, acetone, and NH_3 can effectively change the maximum peaks and the height of the peaks (which are mainly located at about 15.9 eV) for the reflectivity, real dielectric function, and absorption coefficient in various degrees. For example, the value of the maximum peak absorption for the acetone−diazine system is the largest (7.66×10^4 cm^{-1} at 15.92 eV), followed by the absorption peak of ethanol (7.50×10^4 cm^{-1} at 15.94 eV), NH_3 (7.20×10^4 cm^{-1} at 15.90 eV), and then the pure monolayer (7.03×10^4 cm^{-1} at 15.96 eV). In general, the strength of influence on the optical properties of the diazine monolayer is decreased in the the order acetone, ethanol, and NH_3. These results indicate that acetone, ethanol, and NH_3 gases can be easily distinguished one from each other via measuring the optical properties of the diazine monolayer before and after acetone,

ethanol, and NH_3 adsorption, further confirming that the diazine monolayer as gas sensor has high selectivity.

Moreover, the recovery time is also a very important parameter for a good gas sensor, as a long recovery time indicates that desorption of molecules from the gas-sensing materials could be very difficult, and thereby limits the reuse of the materials. Thus, we used the equation $\tau = \nu_0^{-1} e^{-E_{ads}/kT}$ to estimate the recovery time (τ). In the equation, ν_0 is the molecule-attempted frequency. We assume that the attempted frequencies of all molecules have the same order of magnitude as the NO_2 molecules (10^{12} s^{-1} at 300 K).[49,50] The calculated recovery time of the molecules at room temperature (300 K) are listed in Tables 1 and 2. The calculated recovery time of the diazine monolayer for acetone, ethanol, and NH_3 is 7.7 μs, 0.11 ms, and 1.2 μs, respectively, which indicates that the recovery time at room temperature is quite short. Thus, the diazine monolayer can be used as a reusable sensor at room temperature for detection of acetone, ethanol, and NH_3. Further, to have a comparable insight into the sensing properties of the diazine monolayer for NH_3, acetone, and ethanol detection, we compared the considered diazine monolayer with other NH_3, acetone, and ethanol sensors reported in literature.[17,19,20,51−54] For NH_3 sensors, based on the generalized analysis of the adsorption energy, transferred charge, the changes in electronic properties, sensitivity, selectivity, and recovery time at 300 K for diazine, C_2N, C_3N, and C_3N_4 monolayers, we found that the diazine monolayer generally has higher NH_3-sensing performance than C_2N,[17] C_3N,[19,20] and C_3N_4[51] monolayers and most of the metal oxides and conducting polymers.[49] Since there are no reports on the acetone- and ethanol-sensing performance of C_2N, C_3N, and C_3N_4 monolayers, we just compared the diazine monolayer sensor with other acetone and ethanol sensors reported in the review literature.[50,51] We found that the sensing performance (such as working temperature, recovery time, sensitivity, and selectivity) of the diazine monolayer for acetone and ethanol detection is much better than that reported in literature reviews.[50,51] Therefore, based on the analysis of sensitivity, stability, selectivity, and recovery time, it is concluded that the diazine monolayer holds a promising potential for use as a room-temperature gas sensor for detecting molecules including acetone, ethanol, and NH_3.

3. CONCLUSIONS

In conclusion, to fully explore the application potential of the diazine monolayer as a room-temperature gas sensor for detecting acetone, ethanol, and NH_3, the adsorption behaviors, electronic properties, and optical properties of CO_2, CO, N_2O, CH_4, H_2, N_2, O_2, NH_3, acetone, and ethanol molecules on the diazine monolayer were investigated using DFT calculations. We found that all of the abovementioned molecules are physically adsorbed on the diazine monolayer with small adsorption energy and transferred charge. The adsorption of NH_3, acetone, and ethanol dramatically modified the electronic and optical properties of the diazine monolayer, such as the obvious change in electrical conductivity and work function, while the adsorption of the other molecules could not tune the electronic and optical properties of the diazine monolayer, indicating that the diazine monolayer is highly sensitive and selective for NH_3, acetone, and ethanol detection. Further, acetone, ethanol, and NH_3 gases can be easily distinguished from one another via measuring the optical properties of the diazine monolayer before and after adsorption. The calculated

recovery time of the diazine monolayer for acetone, ethanol, and NH_3 is 7.7 μs, 0.11 ms, and 1.2 μs, respectively, which indicates that the recovery time at room temperature is quite short. Therefore, based on the analysis of the sensitivity, stability, selectivity, and recovery time, it is concluded that the diazine monolayer has a promising potential for application in room-temperature gas sensors for detecting molecules including acetone, ethanol, and NH_3.

4. COMPUTATIONAL DETAILS

All calculations were carried out using DMOL^3 code[55,56] based on spin-polarized density functional theory (DFT). The exchange-correlation energy was calculated using the generalized gradient approximation (GGA) within the Perdew−Burke−Ernzerhof (PBE)[57] functional. The DFT+D method with the Grimme scheme was adopted to consider the van der Waals forces.[58,59] The double numerical atomic orbital augmented by d-polarization functions (DNP basis set) and density functional semi-core pseudopotentials (DSPP)[60] was used to describe the electron−ion interaction. The Brillouin zone was defined by the Monkhorst−Pack scheme with a mesh size of $10 \times 10 \times 1$.[61] The electron density difference (EDD) and the Hirshfeld charge method were used to analyze the charge distribution. The convergence values for the displacement, energy, and maximum force in structural optimization are 0.005 Å, 1.0×10^{-6} Ha, and 0.002 Ha/Å, respectively. A real-space global orbital cutoff radius of 4.5 Å was chosen for the calculations. A vacuum space of 20 Å was used to avoid interactions between two periodic units. In this work, we used a $2 \times 2 \times 1$ supercell mode of the diazine monolayer, and in order to confirm whether the size of the $2 \times 2 \times 1$ supercell for the diazine monolayer is large enough to avoid the interaction between adsorbed molecules, we also investigated the $3 \times 3 \times 1$ supercell of the diazine monolayer with acetone and ethanol adsorption. We found that the results such as adsorption strength, transferred charge, and electronic and optical properties for acetone and ethanol adsorption on diazine monolayers of different sizes (2×2 and 3×3) are all the same, indicating that the $2 \times 2 \times 1$ supercell mode of the diazine monolayer is large enough to prevent interactions between adjacent molecules, given the fact that the distances between molecules are all greater than about 11 Å in the $2 \times 2 \times 1$ supercell mode.

Further, in order to assess the adsorption strength, the adsorption energy (E_{ads}) was calculated as $E_{ads} = E_{total} - E_{mono} - E_{mol}$, where E_{total} is the total energy of each molecule adsorbed on the diazine monolayer, E_{mono} and E_{mol} are the total energies of the pristine diazine monolayer and the isolated molecule, respectively. Under this definition, a negative adsorption energy portends that the adsorption process is exothermic and energetically favorable.

■ AUTHOR INFORMATION

Corresponding Author

  Yongliang Yong − *School of Physics and Engineering, Henan Key Laboratory of Photoelectric Energy Storage Materials and Applications, Henan University of Science and Technology, Luoyang 471023, China; Provincial and Ministerial Co-construction of Collaborative Innovation Center for Non-ferrous Metal New Materials and Advanced Processing Technology, Luoyang 471023, China;* ⊙ orcid.org/0000-0001-7376-0738; Email: ylyong@ haust.edu.cn

Authors

Xiaojiao Wang − *School of Physics and Engineering, Henan Key Laboratory of Photoelectric Energy Storage Materials and Applications, Henan University of Science and Technology, Luoyang 471023, China*

Wenwen Yang − *School of Physics and Engineering, Henan Key Laboratory of Photoelectric Energy Storage Materials and Applications, Henan University of Science and Technology, Luoyang 471023, China*

Aodi Zhang − *School of Physics and Engineering, Henan Key Laboratory of Photoelectric Energy Storage Materials and Applications, Henan University of Science and Technology, Luoyang 471023, China*

Xiangyi Xie − *School of Physics and Engineering, Henan Key Laboratory of Photoelectric Energy Storage Materials and Applications, Henan University of Science and Technology, Luoyang 471023, China*

Peng Zhu − *School of Physics and Engineering, Henan Key Laboratory of Photoelectric Energy Storage Materials and Applications, Henan University of Science and Technology, Luoyang 471023, China*

Yanmin Kuang − *Institute of Photobiophysics, School of Physics and Electronics, Henan University, Kaifeng 475004, China*

Complete contact information is available at:
https://pubs.acs.org/10.1021/acsomega.1c00432

Notes

The authors declare no competing financial interest.

■ REFERENCES

(1) Li, H.; Zhao, S.; Zang, S.; Li, J. Functional metal−organic frameworks as effective sensors of gases and volatile compounds. *Chem. Soc. Rev.* **2020**, *49*, 6364−6401.

(2) Fine, G. F.; Cavanagh, L. M.; Afonja, A.; Binions, R. Metal oxide semi-conductor gas sensors in environmental monitoring. *Sensors* **2010**, *10*, 5469−5502.

(3) Wagner, T.; Haffer, S.; Weinberger, C.; Klaus, D.; Tiemann, M. Mesoporous materials as gas sensors. *Chem. Soc. Rev.* **2013**, *42*, 4036−4053.

(4) Zhang, J.; Liu, X.; Neri, G.; Pinna, N. Nanostructured materials for room-temperature gas sensors. *Adv. Mater.* **2016**, *28*, 795−831.

(5) Yong, Y.; Su, X.; Cui, H.; Zhou, Q.; Kuang, Y.; Li, X. Two-dimensional tetragonal GaN as potential molecule sensors for NO and NO_2 detection: A First-Principle Study. *ACS Omega* **2017**, 8888−8895.

(6) Hashtroudi, H.; Mackinnon, R. I. D.; Shafiei, M. Emerging 2D hybrid nanomaterials: towards enhanced sensitive and selective conductometric gas sensors at room temperature. *J. Mater. Chem. C* **2020**, *8*, 13108−13126.

(7) Buckley, D. J.; Black, N. C. G.; Castanon, E. G.; Melios, C.; Hardman, M.; Kazakova, O. Frontiers of graphene and 2D material-based gas sensors for environmental monitoring. *2D Mater* **2020**, *7*, No. 032002.

(8) Meng, Z.; Stolz, R. M.; Mendecki, L.; Mirica, K. A. Electrically-transduced chemical sensors based on two-dimensional nanomaterials. *Chem. Rev.* **2019**, *119*, 478−598.

(9) Donarelli, M.; Ottaviano, L. 2D Materials for gas sensing applications: A review on graphene oxide, MoS_2, WS_2 and phosphorene. *Sensors* **2018**, *18*, No. 3638.

(10) Khan, K.; Tareen, A. K.; Wang, L.; Aslam, M.; Ma, C.; Mahmood, N.; et al. Sensing applications of atomically thin group IV carbon siblings Xenes: Progress, challenges, and prospects. *Adv. Funct. Mater.* **2020**, No. 2005957.

(11) Ferrari, A. C.; Bonaccorso, F.; Falko, V.; Novoselov, K. S.; Roche, S.; Bøggild, P.; et al. Science and technology roadmap for graphene, related two-dimensional crystals, and hybrid systems. *Nanoscale* **2015**, *7*, 4598−4810.

(12) Zhao, Z.; Yong, Y.; Zhou, Q.; Kuang, Y.; Li, X. Gas-sensing properties of the SiC monolayer and bilayer: A density functional theory study. *ACS Omega* **2020**, *5*, 12364−12373.

(13) Liu, X.; Ma, T.; Pinna, N.; Zhang, J. Two-dimensional nanostructured materials for gas sensing. *Adv. Funct. Mater.* **2017**, *27*, No. 1702168.

(14) Anichini, C.; Czepa, W.; Pakulski, D.; Aliprandi, A.; Ciesielski, A.; Samorì, P. Chemical sensing with 2D materials. *Chem. Soc. Rev.* **2018**, *47*, 4860−4908.

(15) Yuan, W.; Shi, G. Graphene-based gas sensors. *J. Mater. Chem. A* **2013**, *1*, 10078−10091.

(16) Varghese, S. S.; Lonkar, S.; Singh, K. K.; Swaminathan, S.; Abdala, A. Recent advances in graphene based gas sensors. *Sens. Actuators, B* **2015**, *218*, 160−183.

(17) Yong, Y.; Cui, H.; Zhou, Q.; Su, X.; Kuang, Y.; Li, X. C_2N monolayer as NH_3 and NO sensors: A DFT study. *Appl. Surf. Sci.* **2019**, *487*, 488−495.

(18) Bhattacharyya, K.; Pratik, S. M.; Datta, A. Controlled pore sizes in monolayer C_2N act as ultrasensitive probes for detection of gaseous pollutants (HF, HCN, and H_2S). *J. Phys. Chem. C* **2018**, *122*, 2248−2258.

(19) Zhao, Z.; Yong, Y.; Hu, S.; Li, C.; Kuang, Y. Adsorption of gas molecules on a C_3N monolayer and the implications for NO_2 sensors. *AIP Adv* **2019**, *9*, No. 125308.

(20) Ma, D.; Zhang, J.; Li, X.; He, C.; Lu, Z.; Lu, Z.; Yang, Z.; Wang, Y. C_3N monolayers as promising candidates for NO_2 sensors. *Sens. Actuators, B* **2018**, *266*, 664−673.

(21) Qiu, H.; Xue, M.; Shen, C.; Zhang, Z.; Guo, W. Graphynes for water desalination and gas separation. *Adv. Mater.* **2019**, *31*, No. 1803772.

(22) Zhang, Y.; Wan, Q.; Yang, N. Recent advances of porous graphene: Synthesis, functionalization, and electrochemical applications. *Small* **2019**, No. 1903780.

(23) Mortazavi, B.; Madjet, M. E.; Shahrokhi, M.; Ahzi, S.; Zhuang, X.; Rabczuk, T. Nanoporous graphene: A 2D semiconductor with anisotropic mechanical, optical and thermal conduction properties. *Carbon* **2019**, *147*, 377−384.

(24) Moreno, C.; Vilas-Varela, M.; Kretz, B.; Garcia-Lekue, A.; Costache, M. V.; Paradinas, M.; et al. Bottom-up synthesis of multifunctional nanoporous graphene. *Science* **2018**, *360*, 199−203.

(25) Freitas, A.; Machado, L. D.; Bezerra, C. G.; Tromera, R. M.; Azevedo, S. Electronic and optical properties of $B_xC_yN_z$ hybrid a-graphynes. *RSC Adv* **2019**, *9*, 35176−35188.

(26) Xia, K.; Zhan, H.; Ji, A.; Shao, J.; Gu, Y.; Li, Z. Graphynes: an alternative lightweight solution for shock protection. *Beilstein J. Nanotechnol* **2019**, *10*, 1588−1595.

(27) Yang, C.; Mahmood, A.; Kim, B.; Shin, K.; Jeon, D. H.; Han, J. K.; et al. Enhancing gas sensing properties of graphene by using a nanoporous substrate. *2D Mater* **2016**, *3*, No. 011007.

(28) Kooti, M.; Keshtkar, S.; Askarieh, M.; Rashidi, A. Progress toward a novel methane gas sensor based on SnO_2 nanorods-nanoporous graphene hybrid. *Sens. Actuators, B* **2019**, *281*, 96−106.

(29) Shaban, M.; Ali, S.; Rabia, M. Design and application of nanoporous graphene oxide film for CO_2, H_2, and C_2H_2 gases sensing. *J. Mater. Res. Technol.* **2019**, *8*, 4510−4520.

(30) Yuan, W.; Chen, J.; Shi, G. Nanoporous graphene materials. *Mater. Today* **2014**, *17*, 77−85.

(31) More, M. P.; Deshmukh, P. K. Computational studies and biosensory applications of graphene-based nanomaterials: A state-of-the-art review. *Nanotechnology* **2020**, *31*, No. 432001.

(32) Barone, V.; Moses, I. A. Structure and stability of graphene-like layers built from heterocyclic units. *Carbon* **2019**, *152*, 128−133.

(33) Dong, M.; Zhang, G.; Li, Z.; Wang, M.; Wang, C.; Fu, X. Anisotropic interfacial properties of monolayer C_2N field effect transistors. *Phys. Chem. Chem. Phys.* **2020**, *22*, 28074−28085.

(34) Ullah, S.; Denis, P. A.; Menezes, M. G.; Sato, F.; Capaz, R. B. Electronic properties of substitutional impurities in graphenelike C_2N, tg−C_3N_4, and hg−C_3N_4. *Phys. Rev. B* **2020**, *102*, No. 134112.

(35) Yar, M.; Hashmi, M. A.; Ayub, K. The C_2N surface as a highly selective sensor for the detection of nitrogen iodide from a mixture of NX_3 (X = Cl, Br, I) explosives. *RSC Adv* **2020**, *10*, 31997−32010.

(36) Varunaa, R.; Ravindran, P. Potential hydrogen storage materials from metal decorated 2D-C_2N: an ab initio study. *Phys. Chem. Chem. Phys.* **2019**, *21*, 25311−25322.

(37) Zhu, L.; Xue, Q.; Li, X.; Wu, T.; Jin, Y.; Xing, W. C_2N: an excellent two-dimensional monolayer membrane for He separation. *J. Mater. Chem. A* **2015**, *3*, 21351−21356.

(38) Xu, J.; Mahmood, J.; Dou, Y.; Dou, S.; Li, F.; Dai, L.; Baek, J. 2D frameworks of C_2N and C_3N as new anode materials for lithium-ion batteries. *Adv. Mater.* **2017**, *29*, No. 1702007.

(39) Yar, M.; Shah, A. B.; Hashmi, M. A.; Ayub, K. Selective detection and removal of picric acid by C_2N surface from a mixture of nitro-explosives. *New J. Chem.* **2020**, *44*, 18646−18655.

(40) Yar, M.; Hashmi, M. A.; Khan, A.; Ayub, K. Carbon nitride 2-D surface as a highly selective electrochemical sensor for V-series nerve agents. *J. Mol. Liq.* **2020**, *311*, No. 113357.

(41) Yar, M.; Hashmi, M. A.; Ayub, K. Nitrogenated holey graphene (C_2N) surface as highly selective electrochemical sensor for ammonia. *J. Mol. Liq.* **2019**, *296*, No. 111929.

(42) Hu, S.; Yong, Y.; Li, C.; Zhao, Z.; Jia, H.; Kuang, Y. Si_2BN monolayers as promising candidates for hydrogen storage. *Phys. Chem. Chem. Phys.* **2020**, *22*, 13563−13568.

(43) Su, X.; Guo, Y.; Zhao, Y.; Liu, S.; Li, H. Gas adsorption investigation on SiGe monolayer: A first-principle calculation. *Sensors* **2020**, *20*, No. 2879.

(44) Pan, W.; Qi, N.; Zhao, B.; Chang, S.; Ye, S.; Chen, Z. Gas sensing properties of buckled bismuthene predicted by first-principles calculations. *Phys. Chem. Chem. Phys.* **2019**, *21*, 11455−11463.

(45) Yong, Y.; Su, X.; Zhou, Q.; Kuang, Y.; Li, X. The $Zn_{12}O_{12}$ cluster-assembled nanowires as a highly sensitive and selective gas sensor for NO and NO_2. *Sci. Rep.* **2017**, *7*, No. 17505.

(46) Yong, Y.; Jiang, H.; Li, X.; Lv, S.; Cao, J. The cluster-assembled nanowires based on $M_{12}N_{12}$ (M = Al and Ga) clusters as potential gas sensors for CO, NO, and NO_2 detection. *Phys. Chem. Chem. Phys.* **2016**, *18*, 21431−21441.

(47) Yong, Y.; Cui, H.; Zhou, Q.; Su, X.; Kuang, Y.; Li, X. Adsorption of gas molecules on a graphitic GaN sheet and its implications for molecule sensors. *RSC Adv* **2017**, *7*, 51027−51035.

(48) Li, S. *Semiconductor Physical Electronics*, 2nd ed.; Springer: USA, 2006.

(49) Kong, J.; Franklin, N. R.; Zhou, C.; Chapline, M. G.; Peng, S.; Cho, K.; Dai, H. Nanotube molecular wires as chemical sensors. *Science* **2000**, *287*, 622−625.

(50) Peng, S.; Cho, K.; Qi, P.; Dai, H. Ab initio study of CNT NO_2 gas sensor. *Chem. Phys. Lett.* **2004**, *387*, 271−276.

(51) Faye, O.; Eduok, U.; Szpunar, J. A. Boron-decorated graphitic carbon nitride (g-C_3N_4): An efficient sensor for H_2S, SO_2, and NH_3 capture. *J. Phys. Chem. C* **2019**, *123*, 29513−29523.

(52) Kwak, D.; Lei, Y.; Maric, R. Ammonia gas sensors: A comprehensive review. *Talanta* **2019**, *204*, 713−730.

(53) Amiri, V.; Roshan, H.; Mirzaei, A.; Neri, G.; Ayesh, A. I. Nanostructured metal oxide-based acetone gas sensors: a review. *Sensors* **2020**, *20*, No. 3096.

(54) Dharmalingam, G.; Sivasubramaniam, R.; Parthiban, S. Quantification of ethanol by metal-oxide-based resistive sensors: A review. *J. Electron. Mater.* **2020**, *49*, 3009−3024.

(55) Delley, B. An all-electron numerical method for solving the local density functional for polyatomic molecules. *J. Chem. Phys.* **1990**, *92*, 508−517.

(56) Delley, B. From molecules to solids with the approach. *J. Chem. Phys.* **2000**, *113*, 7756−7764.

(57) Perdew, J. P.; Burke, K.; Ernzerhof, M. Generalized gradient approximation made simple. *Phys. Rev. Lett.* **1996**, *77*, 3865.

(58) Tkatchenko, A.; Scheffler, M. Accurate molecular van der Waals interactions from ground-state electron density and free-atom reference data. *Phys. Rev. Lett.* **2009**, *102*, No. 073005.

(59) Grimme, S. Semiempirical GGA-type density functional constructed with a long-range dispersion correction. *J. Comput. Chem.* **2006**, *27*, 1787−1799.

(60) Hamann, D. R.; Schluter, M.; Chiang, C. Norm-conserving pseudopotentials. *Phys. Rev. Lett.* **1979**, *43*, 1494−1497.

(61) Monkhorst, H. J.; Pack, J. D. Special points for Brillouin-zone integrations- a reply. *Phys. Rev. B* **1997**, *16*, 1748−1749.